Journal of Photochemistry and Photobiology A: Chemistry 215 (2010) 214–222

Contents lists available at ScienceDirect

Journal of Photochemistry and Photobiology A: Chemistry

journal homepage: www.elsevier.com/locate/jphotochem

One- and two-photon time-resolved fluorescence study of neurotransmitter amino acid–5,6-benzocoumarin conjugates

Graham Hungerford[a,*], Linus Ryderfors[b], Maria José G. Fernandes[c], M. Sameiro T. Gonçalves[c], Susana P.G. Costa[c]

[a] HORIBA Jobin Yvon IBH Ltd., Skypark 5, 45 Finnieston Street, Glasgow G3 8JU, UK
[b] Department of Physics, University of Strathclyde, 107 Rottenrow, Glasgow G4 0NG, UK
[c] Centre of Chemistry, Campus de Gualtar, University of Minho, 4710-057 Braga, Portugal

ARTICLE INFO

Article history:
Received 1 June 2010
Received in revised form 6 August 2010
Accepted 20 August 2010

Keywords:
Amino acids
Benzocoumarin
Time-resolved emission spectrum
Two-photon excitation

ABSTRACT

The time-resolved photophysical characterisation of a set of fluorescent conjugates of neurotransmitter amino acids (glutamic acid, tyrosine and β-alanine) based on a methoxylated 5,6-benzocoumarin fluorophore was performed. Both one- and two-photon excitation were employed to excite the fluorophore and the cross-section with wavelength for the two-photon process determined. The photophysical characterisation was supported using a molecular modelling study, which helped elucidate the molecular transitions (by a ZINDO calculation) and differences in the electron density between the HOMO and LUMO in geometry (PM3) optimised structures. The effect of prolonged irradiation of the conjugates was monitored via fluorimetry and differences in the kinetics of the process observed were found to depend on the amino acid employed.

1. Introduction

Amino acids are an important class of biomolecules that play essential roles, both as the building blocks of proteins and as intermediates in metabolism. Glutamic acid, tyrosine and β-alanine are abundant in the central nervous system and are involved in signalling processes. Therefore, the ability to monitor them is important in neurological sciences for studying the chemical mechanisms and the kinetics of synaptic transmission. Glutamate is involved in cognitive functions like learning and memory and is also a precursor for the synthesis of a major inhibitory neurotransmitter, γ-aminobutyric acid [1]. Tyrosine is a precursor of dopamine – a neurotransmitter involved in controlling movement, regulating memory, sexual and reward seeking behaviours and the regulation of pituitary hormones [2]. β-Alanine acts as a physiological transmitter and is the rate-limiting precursor of carnosine, which is a β-alanine–histidine dipeptide present in muscle and brain tissues [3].

The use of photoremovable protecting groups to inhibit the reactivity of chosen molecules has been extensively reported for the convenient and controlled temporal and spatial release of biomolecules (uncaging) [4–6]. Ideally this process should occur rapidly, with a high yield and at wavelengths that are not detrimental to the biological system. One-photon excitation (OPE) using UV light enables tight control over the timing of the excitation of a tag, but the use of two-photon excitation (TPE) [7] offers the possibility of three-dimensional spatial control of the excitation to be exercised. It is also advantageous as the longer wavelengths (lower energy photons) involved can reduce out of focus photo-damage [8] and allows a greater penetration into biological tissue. Recently reported photolabile groups include polycyclic aromatic structures, which are in most cases fluorophores, allowing the process monitoring by fluorescence techniques. However, few have sufficient sensitivity to TPE, although 8-bromo-7-hydroxycoumarin and 8-bromo-7-hydroxyquinoline appear to be promising candidates [9,10] and several coumarin derivatives have also been synthesised with TPE in mind [11–14]. Also a dicoumarin derivate has been proposed as a phototrigger activated via TPE [15]. 5,6-Benzocoumarin derivatives have been shown to undergo photooxidation [16] and their electronic properties along their photophysical characteristics make them promising for use in biological applications [17–19].

Taking these facts into consideration together with our recent research interests relating to the application of fluorescent conjugates based on fused coumarin derivatives in the photorelease of biologically significant molecules, namely neurotransmitters [20–25], it was decided to make use of time-resolved fluorescence techniques to further characterise these systems. The possibility of using TPE as triggering agent for the release of active entities from the corresponding fluorescent conjugate was evaluated. Fluorescence, as well as being an extremely sensitive technique, provides a

* Corresponding author. Tel.: +44 (0) 1412296796; fax: +44 (0) 1412296790.
E-mail address: graham.hungerford@horiba.com (G. Hungerford).

1010-6030/$ – see front matter © 2010 Elsevier B.V. All rights reserved.
doi:10.1016/j.jphotochem.2010.08.020

multiparameter signal that is highly dependent of the fluorophore's local microenvironment. The use of time-resolved fluorescence is advantageous as it is independent of the fluorophore concentration (within limits).

In this work we employed both steady state and time-resolved fluorescence to characterise the photophysical properties of four fluorophore–amino acid ester conjugates (glutamic acid, at the main and side chain carboxylic acid function, tyrosine and β-alanine) intended for photorelease applications. Both one- and two-photon excitation studies were performed and molecular modelling carried out to help support the experimental findings. As well as characterising the conjugates, it was possible to follow the kinetics during prolonged irradiation of the samples by monitoring the fluorescence signal, which elucidated different kinetics depending on the amino acid present. The origin of this behaviour can relate to previously reported photocleavage [24].

2. Experimental

The methoxylated benzocoumarin (MBC) conjugates **1**–**4**, structures for which are illustrated below (Scheme 1), were synthesised as previously reported [24]. All solvents used were of spectrophotometric grade (supplied by Sigma–Aldrich).

2.1. Steady state spectra

Absorption and fluorescence spectra were measured using Perkin Elmer Lambda 2 uv-vis and HORIBA Scientific FluoroLog 3 spectrophotometers respectively. The bandpass on the excitation and emission monochromators of the FluoroLog were set to 1 nm, unless otherwise stated. All measurements were performed at ambient temperature.

2.2. One-photon excitation TCSPC measurements

These were performed using a HORIBA Scientific Fluorocube system. The excitation source was a HORIBA Scientific DeltaDiode pulsed diode laser, emitting at 375 nm and operating up to 16.6 MHz. The emission was collected using a monochromator tuned to 450 nm and detected using a TBX picosecond detection module. A polariser at the magic angle was employed on the emission. The measured instrumental full width at half maximum (FWHM) using a scattering solution was nominally 200 ps, with the laser giving an optical pulse width (FWHM) of nominally 55 ps. Data were analysed using DAS 6 software and fitted to a sum of exponentials according to Eq. (1).

$$I(t) = \sum_{i=1}^{n} \alpha_i \exp\left(\frac{-t}{\tau_i}\right) \quad (1)$$

The pre-exponential components (α_i) are given normalised to unity and errors given as three standard deviations.

Time-resolved emission spectra (TRES) measurements were performed by recording the fluorescence decay at 4 nm wavelength intervals over the range 390–598 nm, with the data recorded for equal time periods. The fifty-three fluorescence decays were then analysed globally by fitting common lifetimes to all of the individual decay curves (iterated together). The most satisfactory fit was obtained when using the sum of three exponentials in all cases. The pre-exponential values for each of the decay components were then plotted versus wavelength and normalised to produce spectrum associated with the lifetime component (decay associated spectra [26]). With the spectra associated with the short-lived component in methanol a peak due to Raman scattering (seen at one wavelength) was removed and 5-point smoothing was applied to the spectra to remove any noise in the data.

2.3. Two-photon excitation

Whereas linear one-photon excitation (OPE) depends on the average laser power, two-photon excitation (TPE) is a non-linear optical process and is largely dependent on the laser peak power. The TPE efficiency of a molecule therefore depends on its two-photon excitation cross-section, $\sigma_2(\lambda)$, as well as properties of the excitation laser beam. The measured TPE fluorescence signal F as a

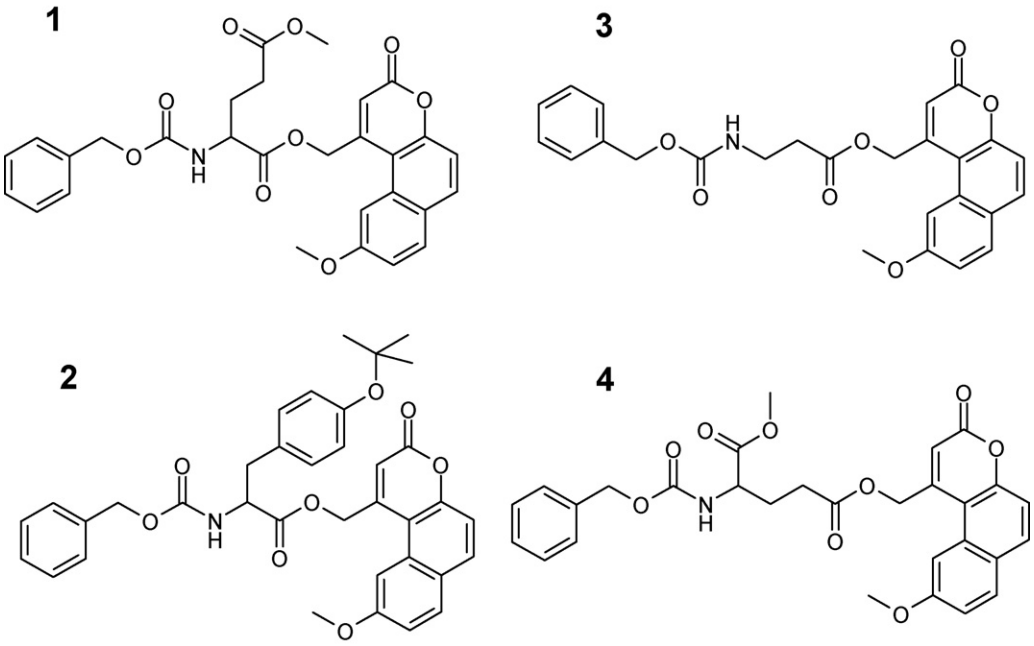

Scheme 1. Structures for the fluorescent neurotransmitter amino acid conjugates **1**–**4**.

function of the excitation wavelength λ can be written as [27].

$$F(\lambda) = A\frac{\sigma_2(\lambda)W^2(\lambda)}{(h\nu)^2\tau(\lambda)x(\lambda)y(\lambda)} \quad (2)$$

A is a parameter independent on λ (including for example the fluorescence collection efficiency) and $W(\lambda)$ is the average laser power, ν is the laser frequency, h is Planck's constant. $\tau(\lambda)$, $x(\lambda)$ and $y(\lambda)$ are, respectively, the FWHMs of the pulse temporal duration and the focal spot size diameters (FWHM), assuming Gaussian laser pulses.

A proper TPE spectrum needs the spectral dependence of the excitation laser beam as described in Eq. (2). An easier way than to measure all the laser beam characteristics in Eq. (2), is to measure the TPE cross-section relative to a reference with known TPE cross-section. Perylene emits and absorbs at similar wavelengths as the benzocoumarin conjugates studied in this paper and is therefore a suitable reference. The unknown TPE cross-section of the benzocoumarins can be determined from Eq. (3) [27].

$$\sigma_{2,s}(\lambda) = \frac{F_s(\lambda_{reg})C_r\varphi_r(\lambda_{reg})}{F_r(\lambda_{reg})C_s\varphi_s(\lambda_{reg})}\sigma_{2,r}(\lambda) \quad (3)$$

The subscript indicates reference (r) or the unknown sample (s) to be determined. F is the TPE fluorescence intensity, λ_{reg} is the wavelength interval at which the emission is recorded. C is the concentration of the dye and $\varphi(\lambda_{reg})$ is the fluorescence quantum yield at the registration wavelength interval λ_{reg}. It is assumed that the fluorescence quantum yields are the same for OPE and TPE molecules and furthermore are independent of the excitation wavelength. Under this approximation, one can determine $\varphi_r(\lambda_{reg})/\varphi_s(\lambda_{reg})$ using a spectrometer as in Eq. (4),

$$\frac{\varphi_r(\lambda_{reg})}{\varphi_s(\lambda_{reg})} = \frac{1-10^{-(OD)_s}}{1-10^{-(OD)_r}}\cdot\frac{\widetilde{F}_r(\lambda_{reg})}{\widetilde{F}_s(\lambda_{reg})} \quad (4)$$

where $(OD)_{s,r}$ is the optical density of the sample and reference at a chosen OPE excitation wavelength of 374 nm. $\widetilde{F}_{r,s}(\lambda_{reg})$ is the measured fluorescence intensities using this excitation wavelength and the same registration wavelength interval as in the TPE measurements.

2.4. Two-photon excitation TCSPC measurements

Time-resolved measurements were obtained on a HORIBA Scientific FluoroCube equipped with a Coherent Chameleon Ti:sapphire laser, operating at 750 nm with 80 MHz repetition rate, for excitation. The emission was collected through a FES 650 nm short pass filter and a blue green copper sulphate filter and was detected at magic angle using a TBX detector. The stop signal for the TAC was obtained from a signal synchronised with the laser pulses and operated at 4 MHz. The instrumental FWHM was 170 ps and the data were modelled with exponential decay functions and analysed using DAS6.

2.5. Two-photon excitation spectra

Two-photon excitation spectra are obtained using fluorescence detection with respect to the tabulated values of the cross-section for perylene, outlined in [27]. The raw data were obtained as counts per second incident on the TBX detector. The differential fluorescence yield in the observation wavelength region was estimated by one-photon excitation using the 375 nm DeltaDiode laser and using the same conditions as in the two-photon excitation studies. The registered detector counts were taken as a measure of the fluorescence intensity of the samples. Estimates for the extinction coefficients for conjugates **1**–**4** were taken from a previous report [24] and for perylene, in dichloromethane, the value of 38,500 cm^{-1} M^{-1} was used.

2.6. Prolonged irradiation study

Time course steady state fluorescence measurements and lifetime determination were performed using a FluoroLog 3 TCSPC spectrophotometer, equipped with a 450 W xenon lamp for steady state excitation. The excitation wavelength was 275 nm, with a bandpass of 10 nm and the emission was monitored at 440 nm with a bandpass of 1 nm. From integration of the spectral output of the Xe lamp a corresponding power estimate of ~2.9 W is obtained for these conditions. A neutral density filter (ND2) was placed on the emission side to reduce the light intensity incident on the detector. The apparatus was run in S/R mode to account for any fluctuation in the intensity of the xenon lamp. These conditions were used for each compound. Data were treated by dividing the initial value (or peak intensity close to the experiment commencement) and the rates were obtained by a linear fit to the data using Microcal Origin 8 software. Time-resolved measurements were performed using either a N-280 or N-340 NanoLED excitation source and timing made using a FluoroHub controlled via DataStation software. Analysis was made using the DAS6 global analysis module, linking the lifetimes.

2.7. Molecular modelling

Semi-empirical quantum chemical calculations were performed using ArgusLab 4.0.1 from Mark Thompson, Plenaria Software LLC of Seattle. Structure geometry was optimised using a PM3 model, as was the determination of the molecular orbitals. The absorption spectra were calculated using the ZINDO routine supplied in the software.

3. Results and discussion

3.1. One-photon excitation

The steady state fluorescence and absorption spectra for the compounds in chloroform are shown in Fig. 1. Previously the photophysical parameters, such as fluorescence quantum yield, peak absorption and emission wavelengths have been reported for these compounds in ethanol [24]. From the figure it can be seen that the peak absorption (349 nm) is the same for all compounds and this can be related to the MBC fluorophore. Differences between the compounds can be seen below 300 nm, relating to the different amino acid residue. The fluorescence emission wavelengths of conjugates **3** and **4** are slightly shorter (437 nm) than those of **1** and **2** (440 nm) and may reflect the influence of the different amino acids. The absorption wavelengths are in keeping with those of the study using ethanol as a solvent [24], while the peak fluorescence is shifted to shorter wavelength, reflecting the effect of lower dielectric constant of chloroform. This type of solvatochromic behaviour has also been reported for other 5,6-benzocoumarin derivatives [17].

ZINDO calculations [28,29] to estimate the electronic absorption spectrum were performed for the compounds and the dielectric constant varied between the extremes of vacuum and water. A calculation of the expected photocleavage product of the fluorophore was also made and the outcome of these calculations is illustrated in Fig. 1. This shows that for the conjugated compounds the spectra are only marginally different for each dielectric constant, with two main transitions between 320 nm and 335 nm obtained at low dielectric constant (Fig. 1b). These both have similar oscillator strengths. At the higher dielectric constant (Fig. 1c) the transitions are shifted to longer wavelengths and compound **2** exhibits the larger oscillator strength. The longer wavelength transitions are enhanced at the expense of those between 325 nm and 330 nm. The

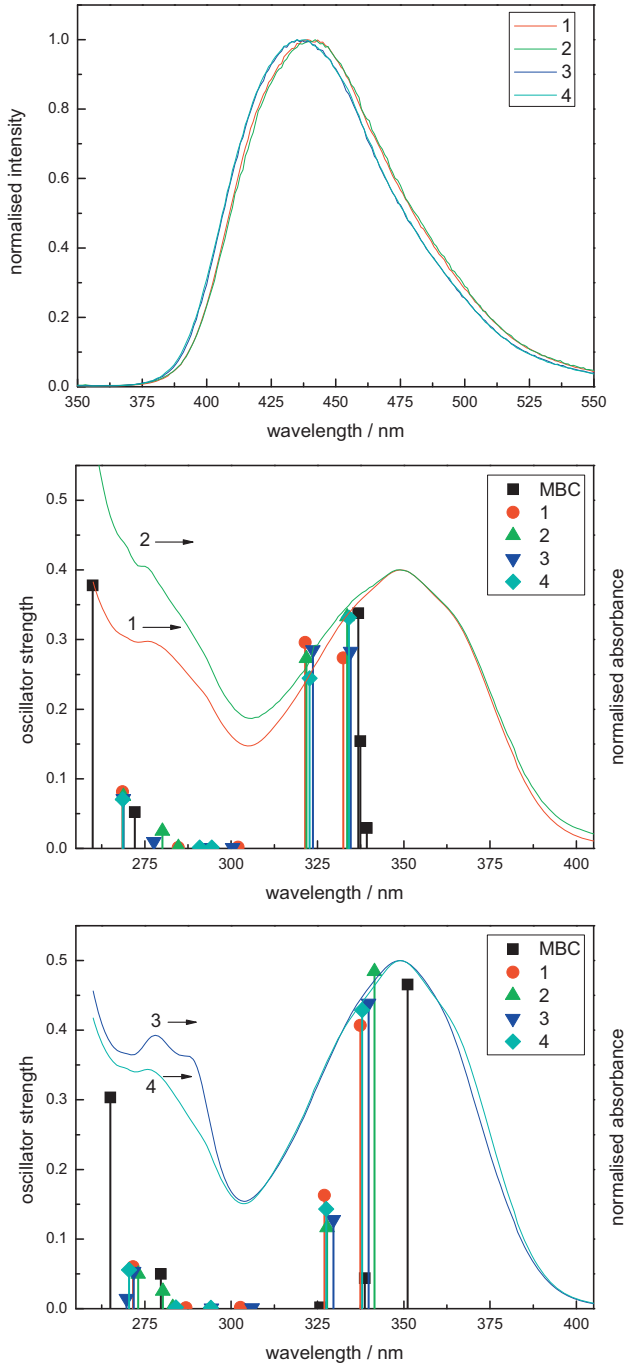

Fig. 1. (a) Normalised fluorescence spectra for conjugates **1**–**4** in chloroform. The lower panels show the oscillator strengths obtained from a ZINDO calculation, (b) in vacuum, (c) in water, for conjugates **1**–**4** and the expected cleaved fluorophore (MBC). The normalised absorption spectra of the conjugates (**1**–**4**) in chloroform are also shown for comparison, **1** and **2** in (b), **3** and **4** in (c).

wavelengths recovered in this study appear sensible in relation to those obtained for the actual molecules in solution. The effect of increasing the dielectric constant on a model of the cleaved MBC fluorophore produces a steady shift to longer wavelengths accompanied by an increase in oscillator strength. This information can help in this study using chloroform and methanol as solvents as well as for future studies and application to proteins.

Time-resolved measurements were performed, exciting into the longer wavelength side of the MBC absorption band, at 375 nm – a wavelength equivalent to that applied later in the TPE study. The lifetimes recovered are shown in Table 1. The decay parameters for the compounds in chloroform appear comparable, with the sum of two exponential components required in order to produce a satisfactory fit to the data. It appears that the results from **3** and **4** are near identical in this solvent. The lifetimes obtained for **2** are slightly longer than those obtained for the other compounds and the relative amount of the fluorescing components are equal. The others have a dominance of the longer-lived decay component.

When using methanol as a solvent, the kinetic behaviour changes, and in order to obtain a satisfactory fit a further exponential component is required. The recovered decay parameters for the compounds all have a significant amount of a fast decay component in the order of 100 ps. The kinetic behaviour is dominated by a longer-lived decay with a lifetime between 6 ns and 7 ns. In all cases there was a minor quantity of a lifetime in the order of 2–3 ns. As with using chloroform as the solvent the time-resolved kinetic for compounds **3** and **4** are similar. Compound **2** again appears slightly different as it has proportionally more of a 3 ns lifetime than the other compounds and the longer-lived decay (6.12 ns) is significantly shorter than the values recovered for the remaining compounds.

The difference in decay kinetics between the two solvents can relate to the influence of the solvent polarity and even the presence of the hydroxyl group in methanol. In order to obtain further information time-resolved emission spectra were recorded for each compound in the two solvents. The resulting decays for each compound were analysed globally and the normalised pre-exponential values plotted for each fluorescence lifetime to produce decay associated spectra [26]. The result of this analysis is shown in Fig. 2. When all the decays (53 in total, covering 390–598 nm at 4 nm intervals) are considered, in order to fit all acceptably a sum of three (common) decay components was required. If chloroform is used as a solvent a short-lived decay component appears with a peak about 415 nm. The presence of this extra component, uncovered by this form of analysis, is testament to the number of decay curves analysed and the wavelength range covered, which explains why this decay is not seen in the simple analysis. For compound **2** this shorter-lived decay time is 86 ps, but for the other compounds this value is nearly twice as long. The other lifetimes are similar to those obtained from the single decay analysis. Using methanol as the solvent the analysis recovered a very short lived species and the same number of decay components as in the simple analysis.

It is noticeable that the short-lived decay is at shorter wavelengths (higher energies) with the longer-lived decay associated

Table 1
Time-resolved data for compounds **1**–**4** in chloroform (C) and methanol (M) with excitation at 375 nm and emission at 450 nm.

Compound	Solvent	τ_1/ns	τ_2/ns	τ_3/ns	α_1	α_2	α_3	χ^2
1	C	1.09 ± 0.04	2.72 ± 0.01		0.37	0.63		1.06
	M	0.10 ± 0.03	2.91 ± 0.90	6.65 ± 0.03	0.41	0.05	0.54	1.02
2	C	1.27 ± 0.03	2.94 ± 0.01		0.50	0.50		1.02
	M	0.15 ± 0.02	3.09 ± 0.33	6.12 ± 0.03	0.36	0.15	0.49	1.06
3	C	0.98 ± 0.03	2.61 ± 0.01		0.31	0.69		1.04
	M	0.08 ± 0.02	1.83 ± 0.21	6.97 ± 0.02	0.40	0.03	0.57	1.04
4	C	0.98 ± 0.02	2.62 ± 0.01		0.30	0.70		1.03
	M	0.09 ± 0.02	3.17 ± 1.54	7.01 ± 0.03	0.42	0.02	0.56	1.01

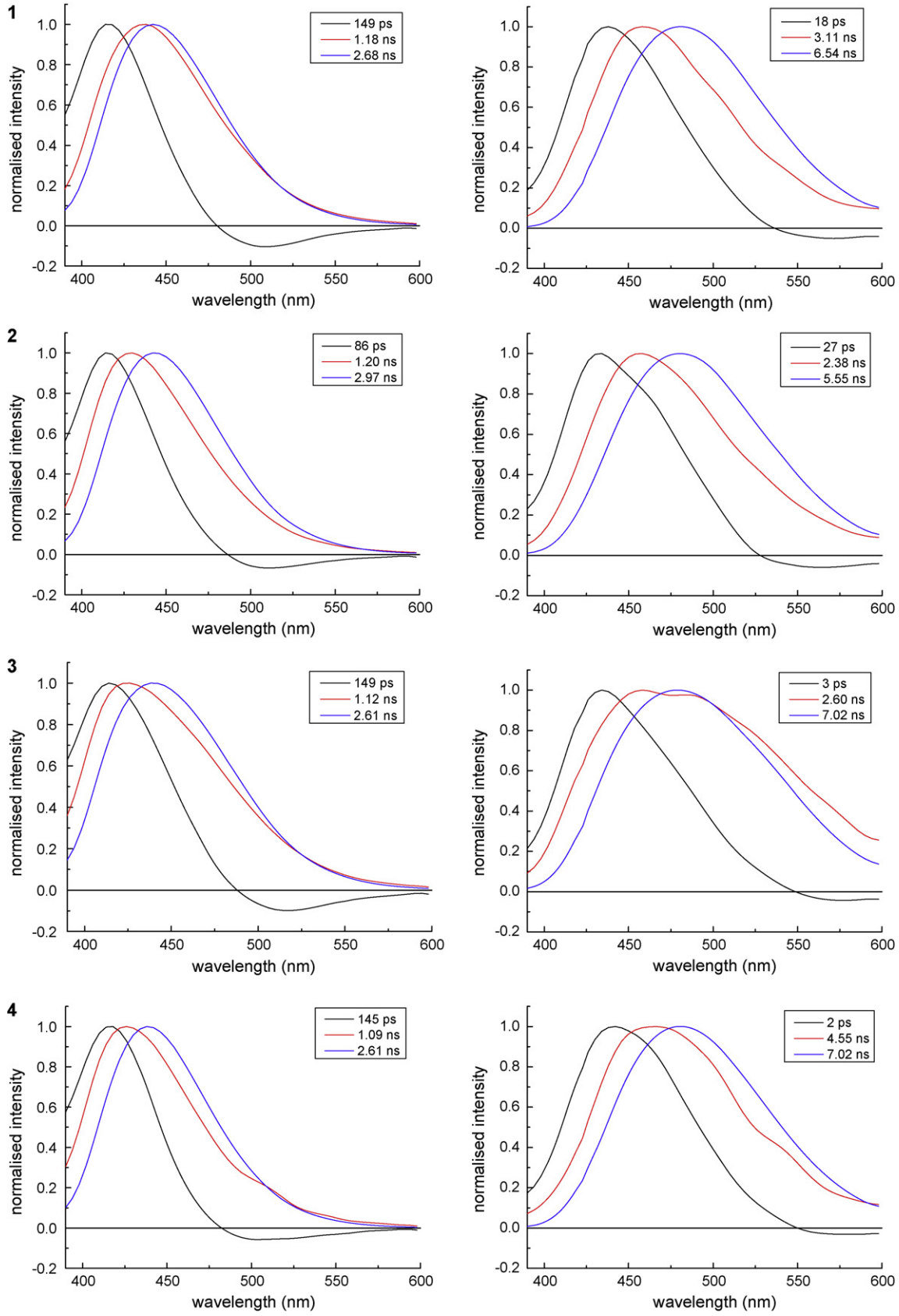

Fig. 2. Outcome of analysis of the TRES measurements for compounds **1**–**4** in chloroform (left) and methanol (right) with 375 nm excitation. This shows the decay associated spectra for the different fluorescing components obtained from the pre-exponential values from global analysis.

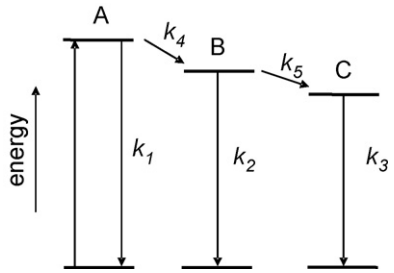

Scheme 2. Potential deactivation pathways for the MBC fluorophore.

with longer wavelengths (lower energies), which points to the fact that the states have the same origin [30]. The wavelengths obtained using methanol as a solvent are longer than those recovered using chloroform in keeping with the effect of solvent relaxation. It should be noted that the value obtained for compounds **3** and **4** for the shortest-lived decay component is beyond the resolution of the equipment and should only be considered as being a very fast decay time. The trend in the longest-lived decay time is the same as that observed in the single curve analysis. These data point to a three-component system with emission from three different energy levels, although from the shape of some of the curves, in terms of breadth and appearance of being the sum of two or more components may indicate some interaction between these levels. A simple scheme (Scheme 2) can be presented to represent possible pathways in the MBC fluorescence.

This assumes that the initial excited (**A**) state, can either relax to the ground state or irreversibly convert to other states (**B** then to **C**). This is similar to schemes proposed for (coumarin-4-yl) methyl derivatives [31–33]. In these works, competition between de-excitation to the ground state and bond cleavage along with a two-step formation of the product has been proposed [33]. It is a moot point to the exact attribution of the states **B** and **C**, but it is likely that they relate to the formation of ion-pair prior to final product formation.

From the lifetime data it is possible to further compare the effect of the amino acid on the MBC conjugate fluorescence. Although not possible to directly obtain the rates of interconversion between the species, an inference can be made from comparing the ratios of the different lifetimes, see Table 2. This shows that the lifetime ratio of the two longer-lived components (τ_3/τ_2) appears mainly independent of conjugate and solvent. However, when the shortest-lived component is considered differences can be easily discerned between the use of the two solvents. The de-excitation/conversion from **A** → **B** is about an order of magnitude faster in the higher polarity methanol than in chloroform. When using chloroform as a solvent the ratios are the same for the compounds, apart from compound **2**. When considering the shortest-lived component, values twice those for the other compounds are found. When using methanol as the solvent, the main differences between compounds **1** and **2** are noted with **3** and **4**, which arises from the short decay time obtained for the latter.

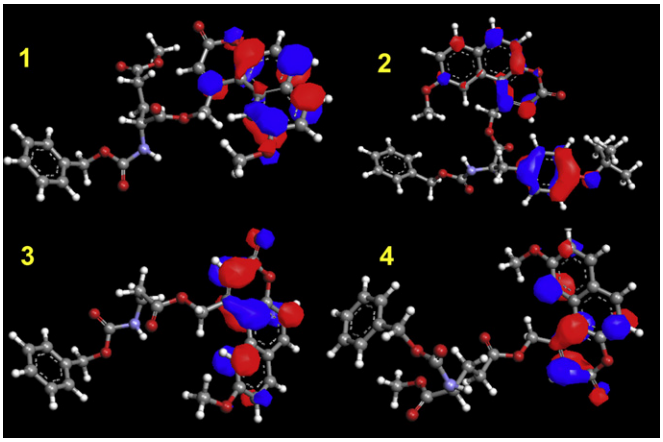

Fig. 3. Difference in electron density between the calculated HOMO and LUMO of **1**–**4**. Red lobes signify negative, blue lobes signify positive. (For interpretation of the references to colour in this figure legend, the reader is referred to the web version of the article.)

Complementary molecular modelling studies were performed on structures geometry optimised using a semi-empirical PM3 model [34]. The difference in electron density between the highest occupied molecular orbital (HOMO) and the lowest unoccupied molecular orbital (LUMO), for each of the compounds, is illustrated in Fig. 3. This indicates that for all the compounds, with the exception of **2**, a transition between the HOMO and the LUMO is predominantly localised on the MBC moiety. This observation is in keeping with another study showing the π–π^* characteristic of the frontier orbitals [17]. For **2**, this is spread between the MBC and tyrosine parts of the conjugate. The electrostatic potential (ESP) mapped onto the electron density of the compounds was calculated and shown in Fig. 4. It is clear from this calculation that the ESP of compound **2** is different to that of the other compounds, with most negative potential on the tyrosine part of the molecule. For the other three compounds the most negative ESP is located on the MBC. The aromatic side chain of tyrosine is known to participate in electron transfer reactions in proteins [35,36] and in this case its electronic properties may help clarify the charge distribution, which can in turn help to explain the fluorescence decay kinetics of this derivative.

3.2. Two-photon excitation

TPE studies of conjugates **1**–**4** were performed in a region where the fluorescence signal showed an intensity squared dependence on the incident laser irradiation power. This dependence is exemplified in Fig. 5 for **1** in chloroform using 750 nm excitation and indicates that the fluorescence is indeed obtained from a two-photon excitation process (see Eq. (2)) [37]. The fluorescence decay parameters obtained from TPE of the conjugates in chloroform using 750 nm excitation are reported in Table 3. As with the one-photon excitation data, the data fitted well to the sum of two

Table 2
Ratios of the lifetime values for **1**–**4** in chloroform and methanol recovered from global analysis of the TRES data. It should be noted that $\tau_1 = (k_1 + k_4)^{-1}$, $\tau_2 = (k_2 + k_5)^{-1}$ and $\tau_3 = k_3{}^{-1}$, given in Scheme 2.

Compound	Solvent					
	Chloroform			Methanol		
	τ_3/τ_1	τ_3/τ_2	τ_2/τ_1	τ_3/τ_1	τ_3/τ_2	τ_2/τ_1
1	18.0	2.3	7.9	363	2.1	173
2	34.5	2.5	14.0	206	2.3	88
3	17.5	2.3	7.5	2340	2.7	867
4	18.0	2.4	7.5	3510	1.5	2275

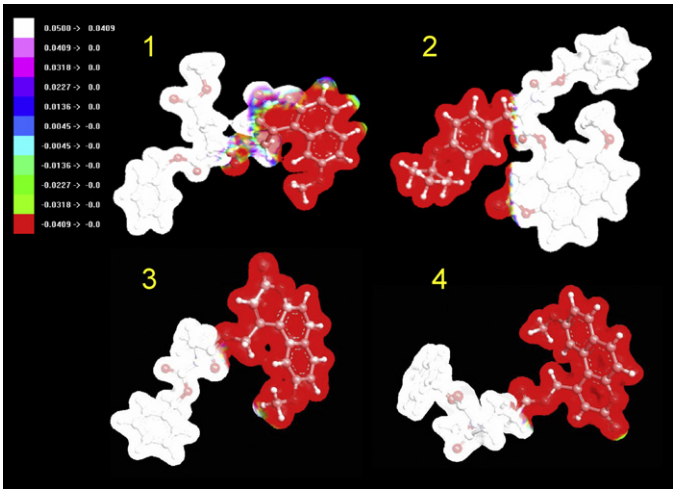

Fig. 4. Mapped surfaces showing the calculated electrostatic potential (ESP) for the conjugates **1**–**4**.

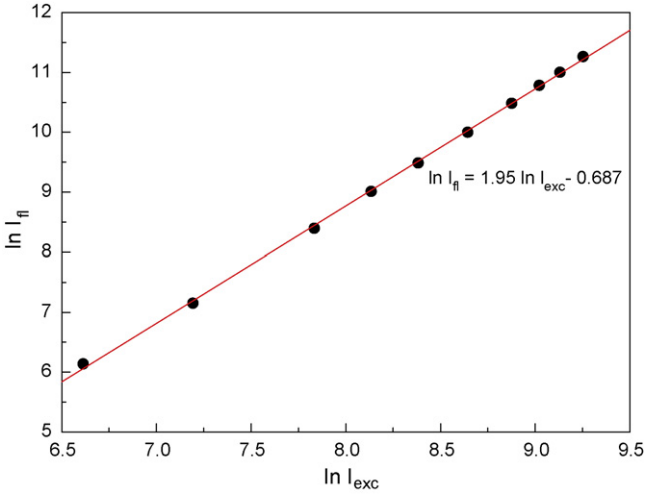

Fig. 5. Quadratic dependence on excitation power for **1** in chloroform, demonstrating a two-photon excitation process.

exponentials and the recovered parameters are in agreement with those for the single curve analysis given in Table 1.

Two-photon excitation spectra of conjugates **1**–**4** in the 730–820 nm region are shown in Fig. 6. The spectra are obtained with reference to the signal obtained from perylene, which absorbs and emits light in the same wavelength region [27]. To arrive at the spectra shown in Fig. 6, Eqs. (3) and (4) were employed. The reference TPE cross-section $\sigma_{2,r}(\lambda)$ for perylene in dichloromethane, also plotted in Fig. 6, is taken from the literature [27]. Although, it should be noted that literature values exhibit some variation [38]. As seen in the figure, the compounds **1**–**4** have a strong absorption at the low end of the spectrum (730 nm), corresponding to double the excitation wavelength of the OPE peaks. The TPE fluorescence signal then drops off at higher wavelengths for **1**, **3** and **4**. Interestingly, compound **2** still has a large TPE fluorescence signal above

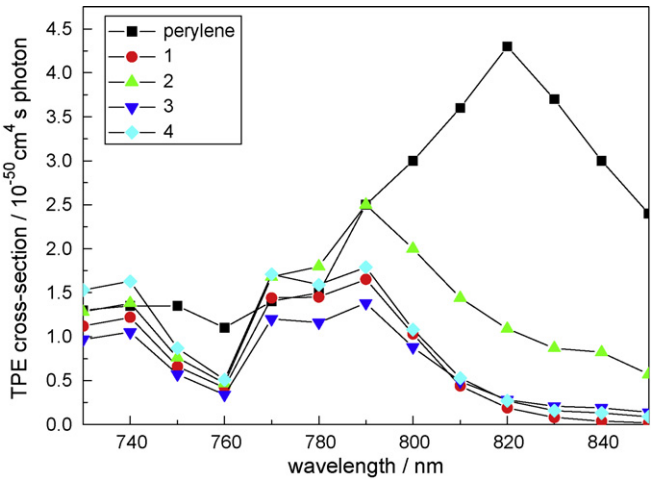

Fig. 6. Two-photon excitation spectra for compounds **1**–**4** in chloroform and the reference data for perylene in dichloromethane.

800 nm. This feature is absent in the OPE spectrum above 400 nm. As can be seen in Fig. 6, the peak TPE cross-sections σ_{max} are in the order of 1–3 Göppert–Mayer units. A value around 1–10 GM seems to be typical for many common dyes [27,39–41]. However, the values that we found are similar to those obtained for other coumarin derivatives [13], although an order of magnitude smaller than those determined for ketocoumarins [12].

3.3. Prolonged irradiation followed using fluorescence

A previous study using irradiation at different wavelengths in a photochemical reactor, monitored by HPLC with a UV detector, showed that compounds **1**–**4** undergo photocleavage [24], with the cleavage products depicted in Scheme 3. The aim of this part of the study was to make use of fluorescence to monitor any cleavage process directly.

This previous study showed a wavelength dependent cleavage rate, so to help gain an insight into the photocleavage process a relatively short wavelength (275 nm) was chosen for excitation. At this wavelength the molecular absorption is principally related to the amino acid part of the conjugate, although the MBC moiety also exhibits some absorption at this wavelength. This is illustrated in Fig. 7, which compares the excitation spectra of compound **2** with uncoupled MBC in chloroform [13]. In the case of **2**, which consists of the fluorescent amino acid tyrosine coupled to the MBC fluorophore, there is the possibility of energy transfer from the tyrosine to MBC, as the tyrosine emission is at ~304 nm [30]. Similar excitation band structures were obtained for all the compounds, with the band centred at 350 nm related to the MBC moiety. As the monitoring wavelength was 440 nm, corresponding to the peak emission of the MBC fluorophore, the choice of these two wavelengths should lead to a reduction in the observed intensity if a cleavage process occurred.

Fig. 8 demonstrates the change in the intensity monitored at 440 nm with 275 nm excitation with time for compounds **1**–**4** in chloroform. Under normal measurement conditions (1 nm band-

Table 3
Time-resolved data for **1**–**4** in chloroform from two-photon excitation.

Compound	τ_1/ns	τ_2/ns	α_1	α_2	χ^2
1	1.29 ± 0.08	2.87 ± 0.03	0.41	0.59	1.12
2	0.97 ± 0.04	2.76 ± 0.05	0.37	0.63	1.02
3	1.11 ± 0.06	2.68 ± 0.13	0.34	0.66	1.00
4	1.16 ± 0.06	2.84 ± 0.14	0.35	0.65	1.02

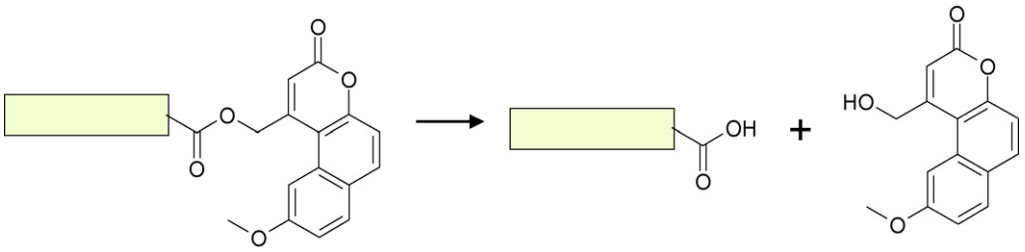

Scheme 3. General illustration of the photocleavage process of compounds **1**–**4**.

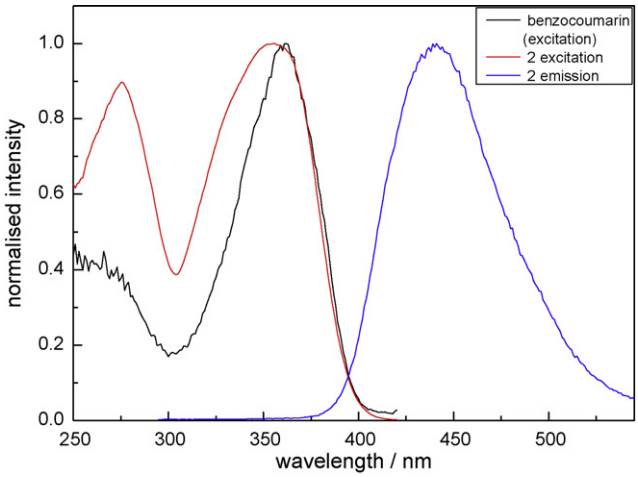

Fig. 7. Excitation and emission spectra of compound **2** in chloroform. Fluorescence was excited at 275 nm and the fluorescence excitation was monitored at 440 nm. The excitation spectrum for uncoupled benzocoumarin is also shown.

pass for both monochromators) no significant change in intensity was observed, as illustrated by the inset in Fig. 8. However by increasing the light intensity incident on the sample (by increasing the excitation monochromator bandpass to 10 nm) a decrease in fluorescence intensity was observed with irradiation time. From this figure it is noticeable that compounds **3** and **4** exhibit the same monotonous decrease (~20%) over the course of the experiment. The rate for which is 2.5×10^{-3} min^{-1}, a value similar in magnitude reported for the compounds in a methanol-buffer solution monitored via HPLC [24] and can indicate that photocleavage may be the dominant process. The behaviour of compounds **1** and **2**, under the same experimental conditions, differs dramatically from that of **3** and **4**. Here it is apparent that the decrease in intensity is a multistep process. Considering **1**, this was visually fitted and an initial rate of 11.2×10^{-3} min^{-1} obtained for the first 25 min and a rate of 4.0×10^{-3} min^{-1} for the remainder of the monitoring period. In the case of **2**, this was visually fitted to three linear regions (0 to ~15 min, 15 to ~53 min and ~53 min to experiment end). The corresponding rates were 21.0×10^{-3} min^{-1}, 7.6×10^{-3} min^{-1} and 4.0×10^{-3} min^{-1}. To specifically elucidate the origin of this behaviour requires further analysis, however it is clear that the electronic coupling between the amino acid and MBC parts of the molecule play a significant role. This coupling is obviously dependent on the structure of the amino acid in the conjugate.

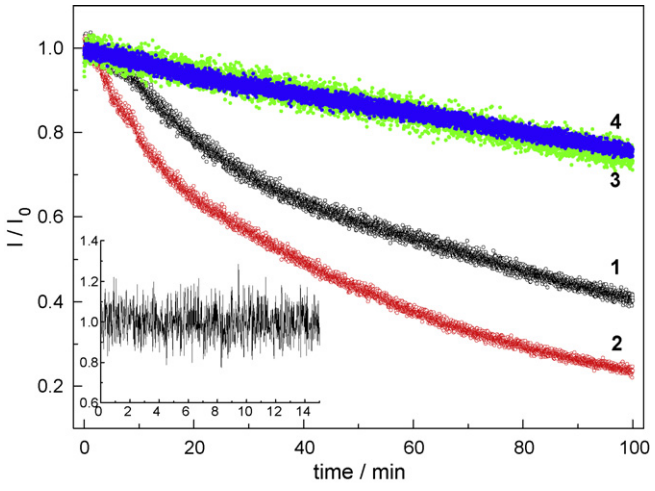

Fig. 8. Fluorescence emission monitored at 440 nm with excitation at 275 nm (bandpass 10 nm) with time. Inset is the response for **3** using an excitation bandpass of 1 nm.

If we concentrate on the enhanced decrease observed with **2**, it is possible to speculate that upon cleavage energy transfer between the tyrosine and MBC moieties is reduced (ceased) as each part is free to migrate away from the other, this is because the excitation wavelength of 275 nm excites the tyrosine and to a lesser extent the MBC. Such a mechanism can explain the faster rate of change observed, which has also been noted in the HPLC study [24]. Other work using different coumarin derivatives has shown that this class of molecule photochemically cleaves forming singlet ion-pair, with the possibility of recombination leading to a multiexponential decay kinetic [31–33].

To ascertain if any effects of irradiation could be seen in the time-resolved fluorescence data, experiments exciting at 280 nm during an irradiation experiment using a FluoroLog TCSPC were performed. In view of the fact that distinct species (amino acid part, MBC moiety) or interactions were expected the data were analysed globally. This involved linking the lifetimes to gain further information concerning the relative concentrations of the emitting species. As with the early global analysis using 375 nm laser excitation, the sum of three linked exponentials was required to fit the dataset. It should be noted that upon prolonged irradiation of the sample with a 375 nm DeltaDiode laser (at an average power of 0.5 mW) no significant changes were seen. However, with an excitation wavelength of 280 nm for the time-resolved measurements a variation in the decay parameters was observed. The outcome is shown pictorially in Fig. 9. This shows that there is a significant increase (~1.5 times) in the amount of intermediate component with irradiation time at the expense of the relative proportion of both the shortest- and longest-lived components. The fact that a change in the lifetime behaviour is observed, along with the previous report using HPLC [24], is indicative that the process also seen in the steady state is not just a simple photobleaching process. A possible explanation for the change in the concentrations of the fluorescing species is that photocleavage inhibits the conversion of state **B** → **C**, producing the reduction in the quantity of the longest-lived decay species, caused by the physical separation of the fluorophore and amino acid moieties.

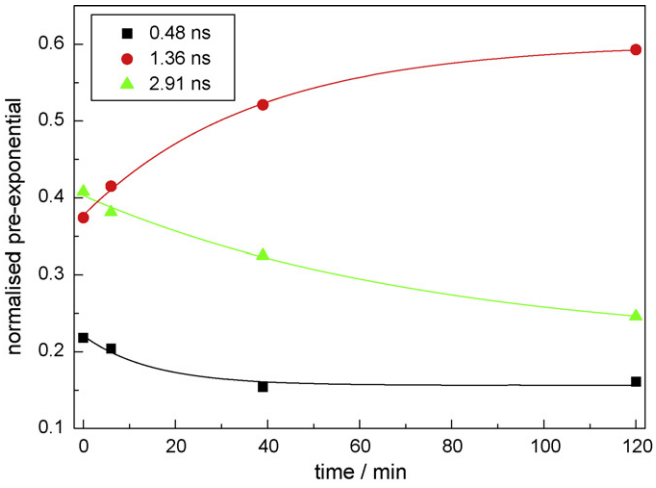

Fig. 9. Outcome of global analysis for **2**, linking three decay times, showing the change in their relative amounts during a prolonged irradiation experiment. Excitation was at 280 nm, emission was at 435 nm.

4. Conclusion

The MBC–amino acid conjugates were studied using both one- and two-photon excitation, with the two-photon excitation cross-sections determined. Time-resolved fluorescence measurements supported by molecular modelling helped elucidate different photophysical behaviour for the tyrosine containing conjugate, which is also reflected in its photocleavage kinetics. This work shows the promise of this class of conjugate for future application, both using OPE and TPE, in the study of the mechanism and kinetics of neurotransmission.

Acknowledgements

The authors wish to thank the *Fundação para a Ciência e Tecnologia* (Portugal) for financial support through project PTDC/QUI/69607/2006 (FCOMP-01-0124-FEDER-007449) and a Ph.D. grant to M.J.G.F. (SFRH/BD/36695/2007).

References

[1] T.A. Kreibich, S.H. Chalasani, J.A. Raper, J. Neurosci. 24 (2004) 7085.
[2] Y. Misu, Y. Goshima, T. Miyamae, Trends Pharmacol. Sci. 23 (2002) 262.
[3] C.A. Hill, R.C. Harris, H.J. Kim, B.D. Harris, C. Sale, L.H. Boobis, C.K. Kim, J.A. Wise, Amino Acids 32 (2007) 225.
[4] A.P. Pelliccioli, J. Wirz, Photochem. Photobiol. 1 (2002) 441.
[5] C.G. Bochet, J. Chem. Soc., Perkin Trans. 1 (2002) 125.
[6] G. Mayer, A. Heckel, Angew. Chem. Int. Ed. 45 (2006) 4900.
[7] J. Bewersdorf, R. Pick, S.W. Hell, Opt. Lett. 23 (1998) 655.
[8] W. Denk, D.W. Piston, W.W. Webb, in: J.P. Pawley (Ed.), Handbook of Biological Confocal Microscopy, Plenum Press, New York, 1995, 445.
[9] T.M. Dore, in: R.S. Givens, M. Goeldner (Eds.), Dynamic Studies in Biology: Phototriggers, Photoswitches, and Caged Biomolecules, Wiley-VCH, Weinheim, Germany, 2005, 435.
[10] Y. Zhu, C.M. Pavlos, J.P. Toscano, T.M. Dore, J. Am. Chem. Soc. 128 (2006) 4267.
[11] Y.-F. Sun, Y.-P. Cui, Dyes Pigments 78 (2008) 65.
[12] X. Li, Y. Zhao, T. Wang, M. Shi, F. Wu, Dyes Pigments 74 (2007) 108.
[13] S. Jockusch, Q. Zheng, G.S. He, H.E. Pudvar, D.J. Yee, V. Balsanek, M. Halim, D. Sames, P.N. Prasad, N.J. Turro, J. Phys. Chem. C 111 (2007) 8872.
[14] S. Härtner, H.-C. Kim, N. Hampp, J. Polym. Chem: Polym. Chem. (2007) 2443.
[15] H.-C. Kim, S. Härtner, N. Hampp, J. Photochem. Photobiol. A: Chem. 197 (2008) 239.
[16] C. Karapire, H. Kolancilar, Ü. Oyman, S. Icli, J. Photochem. Photobiol. A: Chem. 153 (2002) 173.
[17] C. Tablet, M. Hilllebrand, J. Photochem. Photobiol. A: Chem. 189 (2007) 73.
[18] C. Tablet, A. Jelea, M. Hilllebrand, J. Photochem. Photobiol. A: Chem. 183 (2007) 89.
[19] J.A. Key, S. Koh, Q.K. Timerghazin, A. Brown, C.W. Cairo, Dyes Pigments 82 (2009) 196.
[20] A.M. Piloto, D. Rovira, S.P.G. Costa, M.S.T. Gonçalves, Tetrahedron 62 (2006) 11955.
[21] A.S.C. Fonseca, M.S.T. Gonçalves, S.P.G. Costa, Tetrahedron 63 (2007) 1353.
[22] M.J.G. Fernandes, M.S.T. Gonçalves, S.P.G. Costa, Tetrahedron 63 (2007) 10133.
[23] M.J.G. Fernandes, M.S.T. Gonçalves, S.P.G. Costa, Tetrahedron 64 (2008) 3032.
[24] M.J.G. Fernandes, M.S.T. Gonçalves, S.P.G. Costa, Tetrahedron 64 (2008) 11175.
[25] A.M.S. Soares, S.P.G. Costa, M.S.T. Gonçalves, Amino Acids 39 (2010) 121.
[26] L. Davenport, J.R. Knutson, L. Brand, Biochemistry 25 (1986) 1186.
[27] N.S. Makarov, M. Drobizhev, A. Rebane, Opt. Express 16 (2008) 4029.
[28] M.C. Zerner, G.H. Loew, R.F. Kirchner, U.T. Mueller-Westerhoff, J. Am. Chem. Soc. 102 (1980) 589.
[29] M.C. Zerner, in: K.B. Lipkowitz, D.B. Boyd (Eds.), Computational Chemistry II, VCH Publishers Inc., Weinheim, Germany, 1991, Chapter 8.
[30] J.R. Lakowicz, Principles of Fluorescence Spectroscopy, 2nd ed., Kluwer Academic/Plenum Publishers, New York, 1999.
[31] T. Eckardt, V. Hagen, B. Schade, R. Schmidt, C. Schweitzer, J. Bendig, J. Org. Chem. 67 (2002) 703.
[32] R. Schmidt, D. Geissler, V. Hagen, J. Bendig, J. Phys. Chem. A 109 (2005) 5000.
[33] R. Schmidt, D. Geissler, V. Hagen, J. Bendig, J. Phys. Chem. A 111 (2007) 5768.
[34] J.P. Stewart, J. Comp. Chem. 10 (1989) 221.
[35] M. Voicescu, Y. El Khoury, D. Martel, M. Heinrich, P. Hellwig, J. Phys. Chem. B 113 (2009) 13429.
[36] M.K. Manthey, S.G. Pyne, R.J.W. Truscott, Proc. Natl. Acad. Sci. U.S.A. 89 (1992) 1954.
[37] A. Volkmer, D.A. Hatrick, D.J.S. Birch, Meas. Sci. Technol. 8 (1997) 1339.
[38] P.C. Jha, Y. Wang, H. Ågren, Chem. Phys. Chem. 9 (2008) 111.
[39] C. Xu, W.W. Webb, J. Opt. Soc. Am. B: Opt. Phys. 13 (1996) 481.
[40] M.A. Albota, C. Xu, W.W. Webb, Appl. Opt. 37 (1998) 7352.
[41] D.J.S. Birch, Spectrochim. Acta A: Mol. Biomol. Spectrosc. 57A (2001) 2313.